J. Am. Soc. Mass Spectrom. (2017) 28:2500–2507
DOI: 10.1007/s13361-017-1773-1

RESEARCH ARTICLE

Simultaneous Improvement of Resolving Power and Signal-to-Noise Ratio Using a Modified Hadamard Transform-Inverse Ion Mobility Spectrometry Technique

Yan Hong,[1,2] Sheng Liu,[3] Chaoqun Huang,[1] Lei Xia,[1] Chengyin Shen,[1] Haihe Jiang,[1] Yannan Chu[1]

[1]Anhui Province Key Laboratory of Medical Physics and Technology, Center of Medical Physics and Technology, Hefei Institutes of Physical Science, Chinese Academy of Sciences, Hefei, 230031, Anhui, China
[2]School of Electrical and Information Engineering, Anhui University of Science and Technology, Huainan, Anhui 232001, China
[3]College of Computer Science and Technology, Huaibei Normal University, Huaibei, Anhui 235000, China

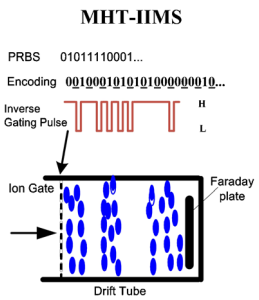

Abstract. In order to improve the resolving power (RP) and signal-to-noise ratio (SNR) of ion mobility spectrometry (IMS) simultaneously, a modified Hadamard transform-inverse ion mobility spectrometry (MHT-IIMS) technique was developed. In this novel technique, a series of isolating codes were appended to each element of the pseudo random binary sequence (PRBS), and then the modified modulation sequence was formed and used to control the ion gate of the inverse IMS (IIMS). Experimental results demonstrate that the MHT-IIMS technique can significantly enhance the resolving power and SNR simultaneously by measuring the spectra of reaction ions. Furthermore, the gas sample CCl_4 and $CHCl_3$ were measured for evaluating the capability of detecting those samples which have single and multiple product ions. The results show that this novel technique is able to simultaneously improve the resolving power and SNR notablely for the real sample detection without any significant instrumental changes.

Keywords: Hadamard transform inverse ion mobility spectrometry, Isolating code, Resolving power, Signal-to-noise ratio

Received: 17 May 2017/Revised: 25 July 2017/Accepted: 27 July 2017/Published Online: 17 August 2017

Introduction

Ion mobility spectrometry (IMS) is a trace chemical substances analytical technology that appeared in the late 1960s to the early 1970s. It has been widely applied to the detection of drugs [1, 2], narcotics [3, 4], explosives [5, 6], and chemical warfare agents [7, 8], owing to its ambient pressure working condition, high sensitivity, analytical flexibility, and real time monitoring capability.

In conventional ion mobility spectrometry, a gas phase sample is ionized, and then the product ions are generated in the reaction region by different ionization sources, such as photoionization, corona discharge, electrospray ionization (ESI), or radioactive ionization. These product ions enter the drift region under the action of the ion gate pulse and are separated due to their different velocities. The velocity of the ions depends on their weight, charge, and shape. The ions in the drift region move toward the Faraday plate and create the ion current signal. The output of the amplified ion signal is synchronized with the ion gate pulse, yielding a mobility spectrum (i.e., a plot of ion current versus time).

The resolving power is one of the key parameters for evaluating the ability of IMS device to separate closely spaced peaks. Generally, the resolving power of IMS is defined as Equation 1 [9].

$$R_p = \frac{t_d}{t_{1/2}} \quad (1)$$

where t_d is the drift time of the single peak and $t_{1/2}$ is the full-width-half-maximum of the single peak in the spectrum of IMS. The resolving power can be calculated on the basis of Equation 2 [10],

Correspondence to: Chaoqun Huang; *e-mail:* cqhuang@aiofm.ac.cn, Yannan Chu; *e-mail:* ychu@aiofm.ac.cn

$$R_p = \frac{1}{\sqrt{\left(\frac{760}{273.15}\right)^2 \frac{t_g{}^2 K_0{}^2 T^2 V^2}{L^4 P^2} + \frac{16 k_B T \ln 2}{qV}}} = \frac{1}{\sqrt{\frac{K^2 t_g{}^2 V^2}{L^4} + \frac{16 k_B T \ln 2}{qV}}} \quad (2)$$

where t_g is the gate pulse width, K is the ion mobility, K_0 is the reduced ion mobility, T is the temperature, V is the voltage, L is the drift tube length, P is the pressure, k_B is Boltzmann's constant, and q is the charge on an electron. Apparently, the resolving power is a complicated function that is related to the temperature and pressure in the drift tube, the gate pulse width, the length of drift region, and the electric field in the drift region. Additionally, the resolving power is also affected by Coulomb repulsion, diffusion of ions, and space charge occurred in the drift region.

The methods and techniques that are utilized to improve the separation power of IMS have been investigated intensively. The resolving power has been enhanced over an order of magnitude by increasing the length of the drift tube [11]. The change of the temperature [12] and pressure [10, 13] in the drift tube has also affected the resolving power. Recently, the increase of the resolving power has been achieved under the non-uniform electric field in the drift region when an alternating current superimposed mode has been applied on the ion gate [14]. Moreover, Tabrizchi and Jazan proposed a new and interesting method to enhance the resolving power via the application of an inverse pulse to the gate grid. Using this technique, 30%–60% higher resolving power was obtained [15].

A signal-to-noise (SNR) is generally accepted for estimating the detection ability of IMS device. The SNR is calculated in Equation 3 [16],

$$SNR = \frac{H}{\sigma} \quad (3)$$

where H is the height of the peak, corresponding to the component concerned, and measured from the maximum of the peak to the extrapolated baseline of the signal, and σ is the standard deviation of the baseline in the spectrum. The higher SNR value means that the limit of detection (LOD) is lower. As for the conventional IMS, the duty cycle is too low (less than 1%) because the ion gate pulse is often small (~200 μs) compared with that of the one total period time (~30 ms). The lower duty cycle restricts the signal level as well as the sensitivity of IMS. One of the methods to improve the SNR and sensitivity of IMS is to raise the ion throughput inside the drift region. Using a modified electrodynamic ion funnel, a 7-fold increase in ion signal has been observed [17]. Moreover, Hadamard transform is a multiplex technique that also can enhance the duty cycle of IMS to 50% and lead to the enhancement of the SNR over the conventional IMS by using a pseudo-random sequence to modulate the ion gate [18, 19].

However, the tradeoff between resolving power and SNR or sensitivity has easily occurred when a certain technique is applied to improve the performance of IMS instrument. Increasing the pulse width of the ion gate can allow more ions to enter into the drift region and increase the signal intensity as well as the sensitivity of IMS. However, a longer opening duration will lead to peak broadening and lower the resolving power. In addition, Hadamard transform technology can improve the SNR as well as the sensitivity of IMS, but it does not possess the ability to alter the resolving power of IMS. Therefore, it often happens that the SNR and the sensitivity of an IMS instrument are sacrificed in order to meet the resolving power requirement, and vice versa. Obviously, a new technique is needed to simultaneously improve the resolving power and the SNR of IMS without compromise between them.

In this report, a modified Hadamard transform technique (MHT) is developed and utilized to control the ion gate of inverse IMS (IIMS). The resolving power and SNR are increased simultaneously over the conventional IMS by measuring the reaction ion. Furthermore, the gas sample CCl_4 and $CHCl_3$ are measured for evaluating their ability to detect those samples that have single and multiple product ions using the MHT-IIMS technique. The results demonstrate that the novel technique is able to simultaneously improve the resolving power and SNR notably without any significant instrumental changes.

Experimental

The homemade atmospheric pressure corona discharge ion mobility spectrometer (APCD-IMS) is demonstrated schematically in Figure 1a. The detailed description about this instrument was shown in our previous work [14, 20]. Briefly, it consists of the ionization region, the reaction region, the Bradbury-Nielson ion gate, and the drift region and data acquisition system.

In the ionization region, the discharge electrodes with the geometry of point to plate were installed coaxially and located at the top of the IMS tube. The reaction ions were generated in this region by means of negative corona discharge through dried air and dragged into the reaction region. Both the reaction and drift regions consist of metal guards that were insulated from each other using Teflon rings. The high voltage through an electric resistance network on the metal rings generated a weak homogeneous electric field along the central axis of the drift tube. At the interface between the reaction and drift region, a Bradbury-Nielson type ion gate is installed and works under the control of an ion gate controller. When the ion gate is opened for a short time, the product ions and the reaction ions swarm into the drift region and drift toward a Faraday plate under the action of the applied homogeneous electric field. Then the current signal will be generated by collecting the ions with a Faraday plate and amplified by a current amplifier (Keithley 428). Subsequently, it is fed into the computer data processing system. The IMS works under negative detection

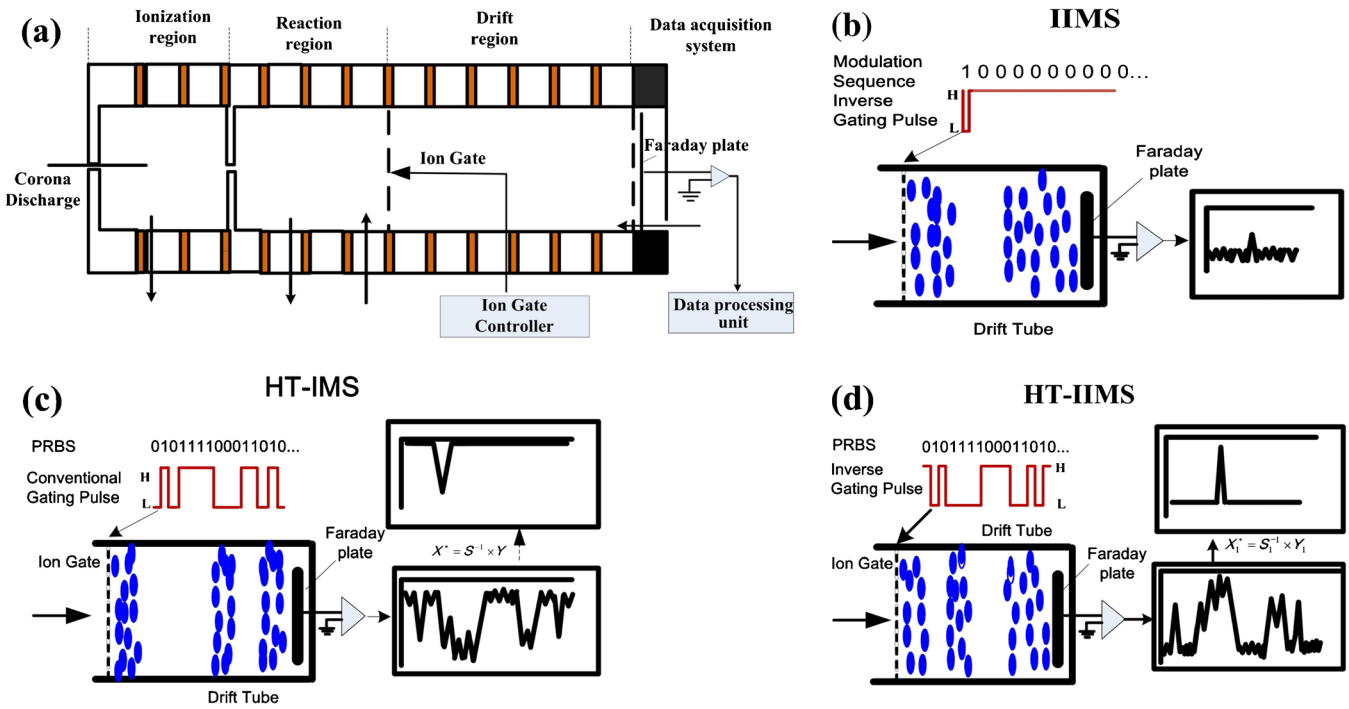

Figure 1. (**a**) Schematic presentation of the atmospheric pressure corona discharge ion mobility spectrometry (APCD-IMS). (**b**) Schematic presentation of the inverse IMS (IIMS). (**c**) Schematic presentation of the HT-IMS. (**d**) Schematic presentation of the HT-IIMS. The ion signal in this figure is a negative detection mode

mode and all the experiments are performed under the condition of 295 K and ambient pressure.

Methodology

Principle of the IIMS, the HT-IMS, and the HT-IIMS

Inverse IMS (IIMS) was developed by Tabrizchi and Jazan in 2010 [15]. In this technique, an inverse pulse was applied to the ion gate and created a dip instead of an ion peak formed in conventional IMS. The control mode of the ion gate is schematically shown in Figure 1b. Note that the negative mode detection is used in all the principle schemata. The symbol "1" corresponds to the low level that is used to close the ion gate, whereas the symbol "0" means the high level is used to open the ion gate. As shown in Figure 1b, the ion gate is opened for a long duration and closed for a short period. Thus, the gate of the IIMS introduces "a dip" into a continuous ion beam instead of ion bundles, so that a 1% duty cycle electronic pulse in inverse mode admits ~99% of the available ion stream. In this case, the ions are distributed outside of the dip and repulse each other. This repulsion effect of charged ions leads to the compression of the dip, namely the improvement of resolving power [21]. The resolving power of the IIMS was enhanced about 30%–60% compared with the conventional IMS.

In Hadamard transform ion mobility spectrometry (HT-IMS), a pseudo random binary sequence (PRBS) is used as the modulation sequence to perform the Hadamard multiplexing. The principle of the HT-IMS is explained briefly in Figure 1c. The convolution of the conventional Hadamard multiplexing is shown in Equation 4 [22, 23],

$$[Y] = [S] \times [X] \tag{4}$$

where Y corresponds to the convolution spectrum that is encoded by multiple normal spectra, S is the $n \times n$ (n is the length of PRBS) matrix that is generated by PRBS, and X corresponds to a series of single spectrums that is derived from a single injection. As for a PRBS, such as "0010001111…", symbol "0" means the low level output that is utilized to close the ion gate, whereas the symbol "1" represents the high level output that is used to open the ion gate. As a result, the convoluted ion signals, which are composed of a series of ion mobility spectra, are obtained under the control of pseudo-random gating function. After the inverse Hadamard transformation, the deconvoluted signal is obtained, and a 2- to 10-fold enhancement in SNR is attained without reduction or improvement in resolving power [18].

The combination of HT technique and IIMS may have the potential power to improve the SNR and resolving power simultaneously as discussed above. Under this consideration, first we tentatively applied the HT technique to control the ion gate of the IIMS, which was named Hadamard transform inverse IMS (HT-IIMS). In this HT-IIMS technique, the modulation sequence (PRBS) is the same as that used in the HT-IMS. However, the symbols "1" and "0"in the PRBS of the HT-IIMS, respectively, mean the low level output that is used to

close the ion gate, and the high level output that is used to open the ion gate. As a result, an inverse ion mobility spectrum will be obtained. The control principle of the HT-IIMS is schematically shown in Figure 1d. It is expected to improve the resolving power and SNR simultaneously using the HT-IIMS technique over the results measured by conventional IMS.

Additionally, the ion signals in the conventional IMS and HT-IIMS mode were all averaged. The duration of data acquisition in the conventional IMS remains almost the same as the scan time of HT-IIMS mode in order to get a better comparison.

Results and Discussion

The Measurements of Reaction Ions Using the Conventional IMS and the HT-IIMS Technique

In this section, only reaction ions produced via negative corona discharge in air were considered. The uniform electric field in the drift region was set as 300 Vcm^{-1}.The ion gate pulse width for all the experiments was 200 μs. As shown in Figure 2a and b, the spectra of reaction ions measured using conventional IMS and HT-IIMS are illustrated. The resolving power and the SNR of these spectra were calculated using the Equations 1 and 3, respectively. Moreover, it is noted that the baseline is distorted by characteristic waveform as shown in Figure 2a. This distortion might be generated by the power supplies, such as high voltage power supply and ion gate power supply, and has negligible effect on our experimental results.

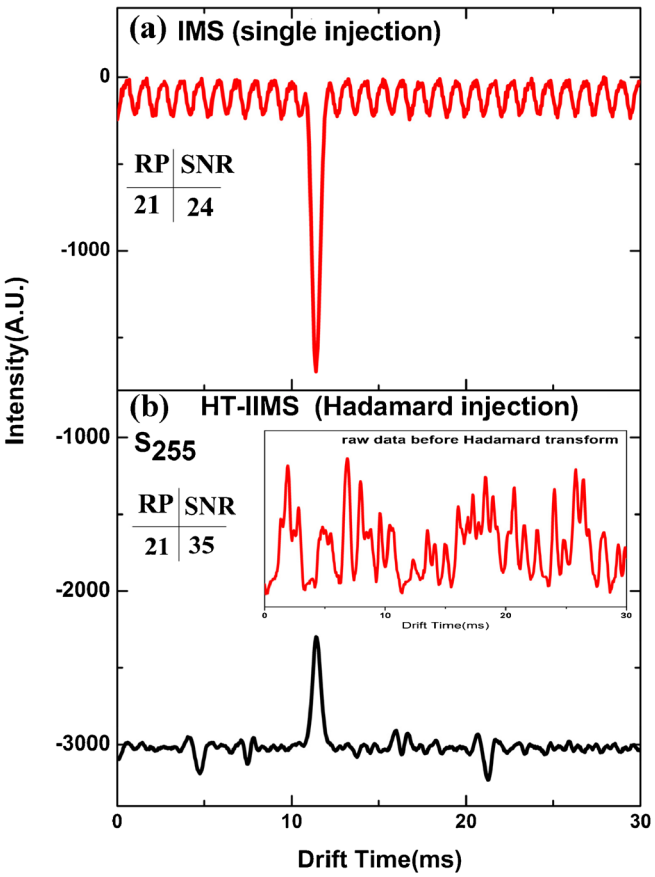

Figure 2. The ion mobility spectra of the reaction ions measured by (**a**) the conventional IMS, (**b**) the HT-IIMS. Here the ion signal in the conventional IMS and in the HT-IIMS were averaged six times and three times respectively, which means the duration of data acquisition (6x30 ms) is close to the scan time 3x51 ms) of the HT-IIMS. Moreover, the ion signal in this figure is a negative detection mode

The resolving power and SNR of the conventional IMS are about 21 and 24 as shown in Figure 2, respectively. It is surprising to note that the resolving power of HT-IIMS is the same as the results measured by the conventional IMS, whereas SNR of the HT-IIMS is 35, which is only 1.46-fold enhancement in comparison to that of the conventional IMS. These results do not meet our initial expectation.

A dip is created in the ion beam rather than generating an ion packet in the IIMS as mentioned above. The ions are distributed outside of the dip and repulse each other. This repulsion effect of charged ions leads to the compression of the dip. However, the convoluted ion signals are composed of multiple irregular dips under HT-IIMS. As shown in the inset plot of Figure 2b, the widths of these dips are non-uniform. Some of them are narrow, while others are wide. Some dips even overlap each other. The repulsion effect among these charged ions is hardly plays a role as it does in the single dip in the IIMS owing to the irregular width of dips and their ambiguous boundaries. As a result, the compression effect of the convoluted ion signals in HT-IIMS suffering a great loss. This is the possible reason for obtaining the same resolving power under conventional IMS and HT-IIMS measurement. As for the SNR, it might also be affected by those irregular dips.

Moreover, some spurious peaks or data artifacts are observed as shown in Figure 2b. A similar phenomenon was also observed by many researches when the HT-IMS technique was utilized [17–19, 24, 25]. Modulation defects were considered as the main source for these spurious peaks. Additionally, Puton and Knap have reported that the shapes of ion swarms at the beginning of drift region may lead to the peak deformation and generate the spurious peaks. The fluctuations of the baseline also make the contribution to those spurious peaks [26]. Parts of the multiplexed ion signal that were most affected by imperfect performance of the BNG have been discarded in order to minimize the effect of modulation defects [18]. Moreover, Prost et al. have developed an effective algorithm to discover and eliminate the data artifacts [25].

The Development of a Modified Hadamard Transform Inverse IMS (MHT-IIMS)

As discussed above, the irregular width and the ambiguous boundaries of dips are supposed to weaken the repulsion effect among the charged ions and make it difficult to improve the resolving power in the HT-IIMS as expected. If this hypothesis were true, the repulsion effect would be a positive effect for

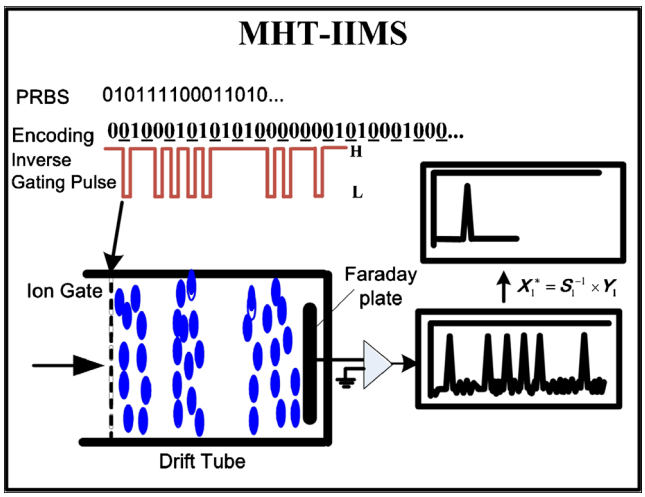

Figure 3. Schematic presentation of the modified Hadamard transform-inverse ion mobility spectrometry (MHT-IIMS)

improving resolving power when each dip in the convoluted ion signals can be separated independently.

In order to separate each dip in the convoluted ion signals, a modified Hadamard transform-inverse ion mobility spectrometry technique (MHT-IIMS) is developed. The principle of this novel MHT-IIMS is demonstrated in Figure 3. Under the MHT-IIMS measurement, the modified modulation sequence is obtained by appending isolating codes to each element of the PRBS. For example, when the modulation PRBS is "010111100011010…", the modified modulation sequence will be encoded as"0 0 1 0 0 0 1 0 1 0 1 0 1 0 0 0 0 0 0 0 1 0 1 0…", where the underlined symbol "0" is the isolating code. In addition, the underline symbol "0" and "0" mean the low level output, which is used to close the ion gate. The symbol "1" means the high level output, which is used to open the ion gate. Under the control of this modified PRBS, the dips will be separated with regular features as shown in Figure 3.

In order to prove the validity of the novel MHT-IIMS technique, the spectra of reaction ions were measured using the MHT-IIMS with different isolating code numbers (from 1 to 3). The experimental results are illustrated in Figure 4a–c, where the order of the S-matrix is 255, the gating pulse width is 200 μs. In comparison to the resolving power and SNR of the conventional IMS, the resolving power and SNR of the MHT-IIMS are improved simultaneously. Additionally, the values of SNR and resolving power increase with the rise of the number of isolating code under the MHT-IIMS mode.

In order to obtain the optimized number of isolating codes for improving resolving power and SNR, the spectra of the reaction ions were measured with the different isolating code numbers.

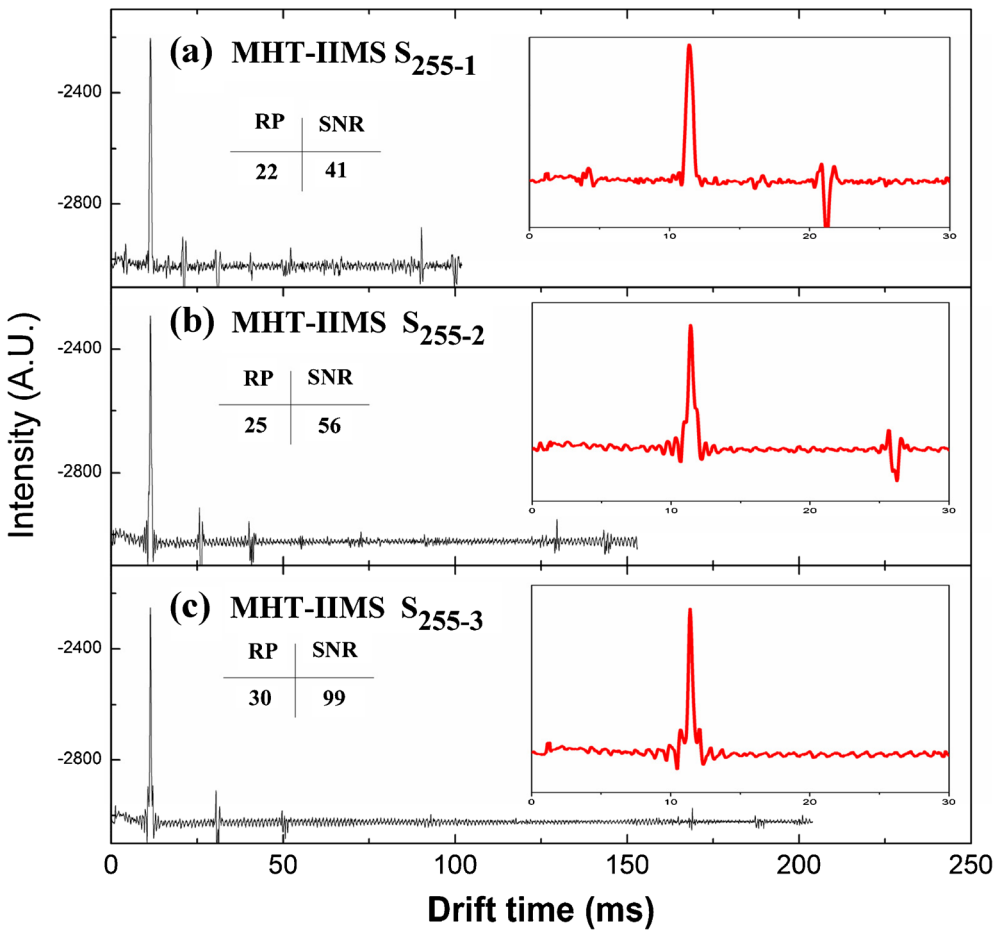

Figure 4. The ion mobility spectra measured by the MHT-IIMS with different isolating code number *n* (**a**) n = 1, (**b**) n = 2, and (**c**) n = 3

Figure 5 shows that the resolving power and SNR were plotted against different isolating code number *n*. With the increase of the isolating code number, the resolving power and SNR increase first, and then become almost constant when isolating code numbers are 3 and 4, respectively, as shown in Figure 5a and b. It is noted that the spectra of the reaction ions were measured three times under the same experimental condition. The values of resolving power and SNR have been calculated using these data. The error bars of the resolving power and SNR were about 2% and 5%, respectively, as shown in this figure, which indicate that our experiment has good reproducibility.

As mentioned above, the irregular width and the unresolved boundaries of the adjacent dips weaken repulsion effect among the charged ions and make it difficult to improve the resolving power in HT-IIMS. However, the convoluted ion signals (dips) are separated gradually under MHT-IIMS measurement with the increase of isolating code number. The ion density on both sides of the dips will be increased accordingly. As a result, the repulsion effect among charged ions distributed on both sides of the dips will be strengthened, which may lead to the further compression of the inverse dips [21]. Thus, the resolving power will be enhanced first as shown in Figure 5a. When the dips were separated completely, the ion density will reach saturation, and the repulsion has no effect on the resolving power.

The modulation defect and unresolved boundary between adjacent signal peaks in convoluted ion signals possibly lead to the spurious peaks in HT-IMS, which could raise the noise level of mobility spectrum, and then result in the loss of the SNR. However, with the increasing number of isolating codes, the convoluted ion signals (dips) are separated gradually, and then the boundary between adjacent signal peaks can be resolved gradually under the MHT-IIMS measurement. The modulation defect was minimized gradually with the separation of adjacent signal peaks. This might be the main reason for fewer artifacts and the improvement of the SNR in MHT-IMS with the increased number of the isolating codes. When the dips are separated completely, the SNR would be constant as shown in the Figure 5b.

On the other hand, it is noted that the duty cycle will be decreased when isolating codes are adopted in the MHT. The gain of the SNR cannot reach the theoretical values because of the decreased duty cycle. Also, the total scan time will be extended. If the order of the S-matrix is 255, the gating pulse width is 200 μs, the total scan time for Hadamard multiplexing will be about 51 ms, and the time consumption for data processing (sampling, A/D conversion, decoding, data presentation) will be about 1.5 s. However, the order of the modulation matrix will be four times (from original 255 to current 1020), the total scan time will also be four times (204 ms) under the MHT measurement, and thus the time cost for data processing will be about 6 s. The time cost is still acceptable for the fast detection speed of the IMS.

As discussed above, the best resolving power and SNR could be obtained when the isolating code numbers are 3 and 4, respectively, under MHT-IIMS measurement. These results indicate that MHT-IIMS is an effective technique to enhance the resolving power and SNR and simultaneously.

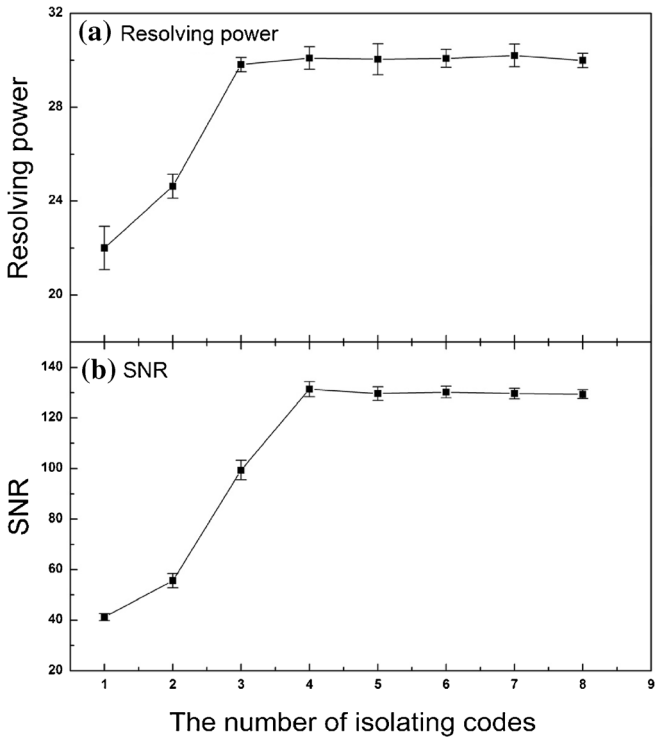

Figure 5. The relationship between (**a**) the resolving power, and (**b**) the SNR and the isolating code number

Sample Detection Using MHT-IIMS Measurement of CCl_4

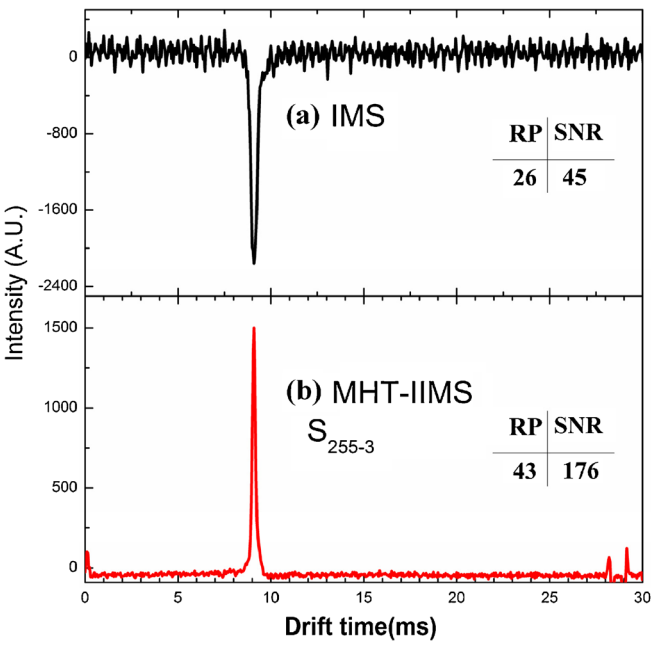

Figure 6. The ion mobility spectra of CCl_4 measured by (**a**) the conventional IMS, and (**b**) the MHT-IIMS. The ion signal was averaged 21 times in conventional IMS mode, whereas the ion signal was averaged three times in MHT-IIMS mode

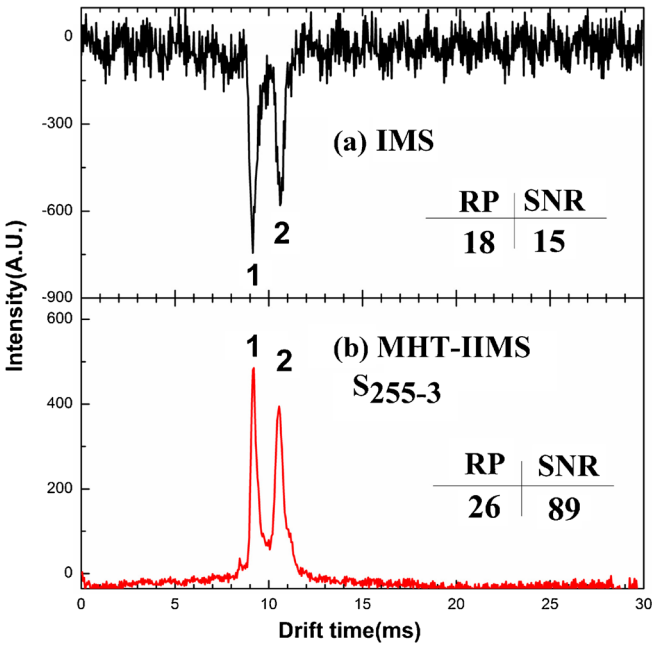

Figure 7. The ion mobility spectra of $CHCl_3$ measured by (**a**) the conventional IMS, and (**b**) the MHT-IIMS The ion signal was averaged 21 times in conventional IMS mode, whereas the ion signal was averaged three times in MHT-IIMS mode

To further evaluate the capability of the novel MHT-IIMS technique, the gas sample CCl_4 was measured by a home-made atmospheric pressure nitrogen corona discharge ion mobility spectrometry apparatus (APNCD-IMS), which can be referred to in our previous report [27]. Different from the APCD-IMS apparatus, an additional curtain region located between the ionization region and the reaction region is used to prevent sample gases from diffusing into the ionization region. In the ionization region, thermal electrons were generated by means of negative corona discharge through nitrogen gas at atmospheric pressure. The gas samples CCl_4 and $CHCl_3$ were introduced into the reaction region by carrier gas N_2 and attached by the thermal low-energy electrons, which were dragged from the ionization region. The product ions were formed by the interaction between the low-energy electrons and the gas sample. The uniform electric field in the drift region is 490 Vcm^{-1}.

Gas sample CCl_4 (~100 ppb) was injected into the IMS cell by syringe pump. The product ions $Cl^-(H_2O)_n$ that were measured by conventional IMS and MHT-IIMS, respectively. are demonstrated in Figure 6. As shown in this figure, the resolving power and SNR under conventional IMS measurement are 26 and 45, respectively. When three isolating codes were appended, the SNR reached 176, which is about 3.9 times over the results measured by conventional IMS. Additionally, the resolving power is 65% higher compared with the result of the conventional IMS.

Measurement of $CHCl_3$

Furthermore, the gas $CHCl_3$ was measured to evaluate its ability to detect those samples which have multiple product ions using conventional IMS and MHT-IIMS, respectively. About 480 ppb gas $CHCl_3$ was injected into IMS cell with the same experimental condition as the measurement of CCl_4. As shown in Figure 7, two product ions (labeled "1" and "2") were observed. Here, the resolving power and SNR were calculated using the peak "1". A 1.4-fold enhancement of resolving power and a 5.9-fold enhancement of SNR were achieved under the MHT-IIMS in comparison to that of the conventional IMS as shown in this figure. It is noted that the accurate assignment of the two products needs further investigation in our next work. Tese results further validate that the MHT-IIMS technique can be used to analyze the complex system with higher SNR and higher resolving power.

Conclusion

In this report, in order to explore an effective mathematical method to improve the resolving power and SNR of IMS simultaneously, a modified Hadamard transform-inverse ion mobility spectrometry (MHT-IIMS) technique was developed for the first time. The resolving power and SNR, respectively, were enhanced simultaneously over the conventional IMS by the measurement of the reaction ion. Furthermore, gas samples CCl_4 and $CHCl_3$ were measured for evaluating their ability to detect those samples that have single and multiple product ions using the MHT-IIMS technique. The results demonstrate that the novel technique is able to simultaneously improve the resolving power and SNR without any significant instrumental changes, although the resolving power in this work was not optimized to the best value.

Acknowledgements

This work is supported by National Natural Science Foundation of China (No. 61671434, 21477132, 21403245).

References

1. Keller, T., Miki, A., Regenscheit, P., Dirnhofer, R., Schneider, A., Tsuchihashi, H.: Detection of designer drugs in human hair by ion mobility spectrometry (IMS). Forensic Sci. Int. **94**, 55–63 (1998)
2. Roscioli, K.M., Tufariello, J.A., Zhang, X., Li, S.X., Goetz, G.H., Cheng, G.L., Siems, W.F., Hill, H.H.: Desorption electrospray ionization (DESI) with atmospheric pressure ion mobility spectrometry for drug detection. Analyst **139**, 1740–1750 (2014)
3. Fuche, C., Deseille, J.: Ion mobility spectrometry: a tool to detect narcotics and explosives. Actual. Chim. 91–95 (2010)
4. McGann, W.: A new, high efficiency ion trap mobility detection system for narcotics. (1997)
5. Ewing, R.G., Atkinson, D.A., Eiceman, G.A., Ewing, G.J.: A critical review of ion mobility spectrometry for the detection of explosives and explosive related compounds. Talanta **54**, 515–529 (2001)
6. Asbury, G.R., Klasmeier, J., Hill, H.H.: Analysis of explosives using electrospray ionization/ion mobility spectrometry (ESI/IMS). Talanta **50**, 1291–1298 (2000)
7. Yang, L., Han, Q., Cao, S.Y., Yang, J., Yang, J.C., Ding, M.Y.: Portable solid phase micro-extraction coupled with ion mobility spectrometry system for on-site analysis of chemical warfare agents and simulants in water samples. Sensors **14**, 20963–20974 (2014)

8. Steiner, W.E., Clowers, B.H., Matz, L.M., Siems, W.F., Hill, H.H.: Rapid screening of aqueous chemical warfare agent degradation products: Ambient pressure ion mobility mass spectrometry. Anal. Chem. **74**, 4343–4352 (2002)
9. Rokushika, S., Hatano, H., Baim, M.A., Hill, H.H.: Resolving measurement for ion mobility spectrometry. Anal. Chem. **57**, 1902–1907 (1985)
10. Davis, E.J., Grows, K.F., Siems, W.F., Hill, H.H.: Improved ion mobility resolving power with increased buffer gas pressure. Anal. Chem. **84**, 4858–4865 (2012)
11. Dugourd, P., Hudgins, R.R., Clemmer, D.E., Jarrold, M.F.: High-resolving ion mobility measurements. Rev. Sci. Instrum. **68**, 1122–1129 (1997)
12. Tabrizchi, M.: Temperature effects on resolution in ion mobility spectrometry. Talanta **62**, 65–70 (2004)
13. Davis, E.J., Dwivedi, P., Tam, M., Siems, W.F., Hill, H.H.: High-pressure ion mobility spectrometry. Anal. Chem. **81**, 3270–3275 (2009)
14. Liu, S., Huang, C.Q., Shen, C.Y., Jiang, H.H., Chu, Y.N.: A novel driving mode for ion shutter based on alternating current superposition and its application to ion mobility spectrometry. Sensor. Actuat. B–Chem. **211**, 102–110 (2015)
15. Tabrizchi, M., Jazan, E.: Inverse ion mobility spectrometry. Anal. Chem. **82**, 746–750 (2010)
16. Cumeras, R., Figueras, E., Davis, C.E., Baumbach, J.I., Gracia, I.: Review on ion mobility spectrometry. Part 2: hyphenated methods and effects of experimental parameters. Analyst **140**, 1391–1410 (2015)
17. Clowers, B.H., Ibrahim, Y.M., Prior, D.C., Danielson, W.F., Belov, M.E., Smith, R.D.: Enhanced ion utilization efficiency using an electrodynamic ion funnel trap as an injection mechanism for ion mobility spectrometry. Anal. Chem. **80**, 612–623 (2008)
18. Clowers, B.H., Siems, W.F., Hill, H.H., Massick, S.M.: Hadamard transform ion mobility spectrometry. Anal. Chem. **78**, 44–51 (2006)
19. Szumlas, A.W., Ray, S.J., Hieftje, G.M.: Hadamard transform ion mobility spectrometry. Anal. Chem. **78**, 4474–4481 (2006)
20. Han, H.Y., Feng, H.T., Li, H., Wang, H.M., Jiang, H.H., Chu, Y.N.: Electron attachment studies for $CHCl_3$ using ion mobility spectrometry. Chin. J. Chem. Phys. **24**, 218–224 (2011)
21. Ilbeigi, V., Tabrizchi, M.: Peak-peak pepulsion in ion mobility spectrometry. Anal. Chem. **84**, 3669–3675 (2012)
22. Kaneta, T., Yamaguchi, Y., Imasaka, T.: Hadamard transform capillary electrophoresis. Anal. Chem. **71**, 5444–5446 (1999)
23. Lin, C.H., Kaneta, T., Chen, H.M., Chen, W.X., Chang, H.W., Liu, J.T.: Applications of Hadamard transform to gas chromatography mass spectrometry and liquid chromatography mass spectrometry. Anal. Chem. **80**, 5755–5759 (2008)
24. Kwasnik, M., Caramore, J., Fernandez, F.M.: Digitally-multiplexed nanoelectrospray ionization atmospheric pressure drift tube ion mobility spectrometry. Anal. Chem. **81**, 1587–1594 (2009)
25. Prost, S.A., Crowell, K.L., Baker, E.S., Ibrahim, Y.M., Clowers, B.H., Monroe, M.E., Anderson, G.A., Smith, R.D., Payne, S.H.: Detecting and removing data artifacts in Hadamard transform ion mobility-mass spectrometry measurements. J. Am. Soc. Mass Spectrom. **25**, 2020–2027 (2014)
26. Puton, J., Knap, A., Siodlowski, B.: Modeling of penetration of ions through a shutter grid in ion mobility spectrometers. Sens. Actuator B–Chem. **135**, 116–121 (2008)
27. Feng, H.T., Niu, W.Q., Han, H.Y., Huang, C.Q., Wang, H.M., Matuska, J., Sabo, M., Matejcik, S., Jiang, H.H., Chu, Y.N.: Rate constants of electron attachment to chlorobenzenes measured by atmospheric pressure nitrogen corona discharge electron attachment ion mobility spectrometry. Int. J. Mass Spectrom. **305**, 30–34 (2011)